Nuclear Instruments and Methods in Physics Research B 117 (1996) 235–242

ELSEVIER

NIM B
Beam Interactions with Materials & Atoms

Energy distributions of hydrocarbon secondary ions from thin organic films under keV ion bombardment: Correlation between kinetic and formation energy of ions sputtered from tricosenoic acid

A. Delcorte *, P. Bertrand

Université Catholique de Louvain, PCPM, 1 Place Croix du Sud, B-1348 Louvain-la-Neuve, Belgium

Received 5 December 1995; revised form received 2 February 1996

Abstract

The kinetic energy distributions (KED) of secondary ions sputtered from tricosenoic acid films under Ga^+ bombardment have been presented recently [1]. Below mass 100, the positive ion spectrum of tricosenoic acid is mainly constituted by the series of $C_xH_y^+$ peaks. Within each $C_iH_y^+$ series, the KED of these ions broadens when the number y of hydrogen atoms decreases. In this paper, we propose a phenomenological model accounting for the characteristic behavior of these ions. It is based on an initial transfer of momentum leading to the emission of an original fragment, reflecting the chemical structure of the target, and followed by a fast reorganization when its internal energy is in excess. Consequently, the ions emitted as a result of a violent collision, carrying a large excess of internal energy, will exhibit both a broad KED and a high degree of reorganization with respect to the structure of the original fragment. This interpretation highlights the effect of the chemical and molecular structure of the organic target on the emission process of the secondary molecular ions. Indeed, this structure determines the nature of the original fragments which have proved their utility for analytical purpose. These fragments lead to intense peaks in the mass spectra, allowing the recognition of the original chemical structure of the samples (fingerprint). In addition, such secondary ions resulting from a direct emission pathway, as suggested by their very narrow KED, turn out to be the best candidates for quantification.

1. Introduction

In static SIMS, the mechanisms by which molecular ions are sputtered from organic films are not very well known yet [2,3]. As low primary ion fluences are required to obtain a molecular information concerning the structure and chemistry of the surface, the operating conditions are soft (fluence $< 10^{13}$ ions/cm^2), corresponding to the 'single-cascade' regime in which collision cascade overlapping can be neglected [4]. This ensures a good reproductibility of the spectra and little or no modification of the surface [5]. Even in these conditions, it seems clear however that one single mechanism cannot account for the emission of atomic ions as well as molecular parent or fragment ions. Several models describing the emission of polyatomic ions under keV ion bombardment have been proposed in the literature (collision cascade [6–14], correlated motion [15,16], vibrational excitation [17,18], recombination in the gas phase [19], etc). Nevertheless, the application of these models to the case of long hydrocarbon-based chains (large organic molecules and polymers) is not straightforward [2]. In particular, the recombination of organic species in the gas phase [19] seems inappropriate to describe the emission of the characteristic secondary ions reflecting the chemical structure of these organic (macro)molecules, which often constitute the most intense peaks of the SI spectra [20]. For these ions, a direct emission process seems more reasonable. Recent MD simulations of the sputtering of small organic adsorbates on Pt show in addition that the ejection of a portion of the intact adsorbate (original fragment), sometimes followed by rearrangement or hydrogen loss, is a very common mechanism of emission compared to the recombination of initially separated molecules, which is much less probable and produces unstable species [21–23]. As an exception to this general rule is mentioned the reactive capture of hydrogen leading to species which are more saturated than the original molecule [23].

In order to determine the kind of mechanism governing the ion formation and emission from polyatomic organic targets, the interpretation of the KED of the secondary ions appearing in their spectra was initiated recently [1,24]. In Ref. [1], a detailed study of the KED of secondary ions

* Corresponding author. Fax +32 10 473452; E-mail: delcorte@pcpm.ucl.ac.be.

PII S0168-583X(96)00306-0

sputtered from a tricosenoic acid bilayer deposited by the Langmuir–Blodgett technique was presented. This compound was chosen mainly for the resemblance between its structure and the one of aliphatic polymers, which is also suggested by a great similarity between the SI spectra. In the particular case of tricosenoic acid, none of the mechanisms quoted above seems appropriate to describe the behavior of the C_xH_y secondary ions, e.g. the relative broadening of the kinetic energy distribution observed in each C_iH_y series when going from the most saturated species to the least saturated one [1]. This is why an interpretation based on the reorganization of the excited C_xH_y ions by hydrogen elimination was proposed to explain this systematic variation. In Ref. [24], two polymers are studied, a commercial PET spin-coated on a Si wafer and a copolymer of fluorinated phenyl-maleimid and vinylether (MV copolymer). The KED of the fingerprint ions of these two polymers [for PET: $C_6H_4^+$ (76 D) and $C_6H_4CO^+$ (104 D); for the MV copolymer: $C_{11}F_3O_2^-$ (242 D) and $C_7H_7O^-$ (107 D)] are very narrow, in comparison with the distribution of less characteristic ions, suggesting that only a soft interaction may lead to their emission as intact species. For these polymers, a similar unsaturation broadening of the C_xH_y secondary ion KED is observed for small ion size ($x \leq 3$), but the interpretation is complicated by the various pathways leading to the formation of these ions in such complex systems. Nevertheless, a similar explanation involving the fragmentation of excited species is not unrealistic.

In the following, an interpretation of the C_xH_y ion KED, associating collisional and reorganization aspects (hydrogen elimination), is developed. It does not account for the shape of the kinetic energy distribution of the C_xH_y ions but for a characteristic parameter which seems relevant, namely the median of the KED.

2. Theoretical considerations

2.1. Diatomic molecule

The sputtering of diatomic molecules has been theoretically described by several authors [9–12]. It can be used as a starting point for the interpretation of the emission of the C_xH_y species. In this work, we consider the case of a single momentum transfer to one atom of the molecule. This assumption is severe but justified as a first approximation by the good correlation obtained with experimental data (see Section 3). For diatomic molecules, it is assumed as initial conditions that a momentum $\boldsymbol{p}$ is transferred to atom 1, while atom 2 is at rest [10,11]. The total energy transmitted to the molecule is then $E = p^2/2m_1$, where m_1 is the mass of atom 1. If the molecule leaves intact, the momentum $\boldsymbol{p}_{cm}$ of its center of mass will be equal to $\boldsymbol{p}$ and the kinetic energy of the center of mass will be:

$$E_{cm} = p_{cm}^2/[2(m_1 + m_2)] = m_1 E/(m_1 + m_2). \quad (1)$$

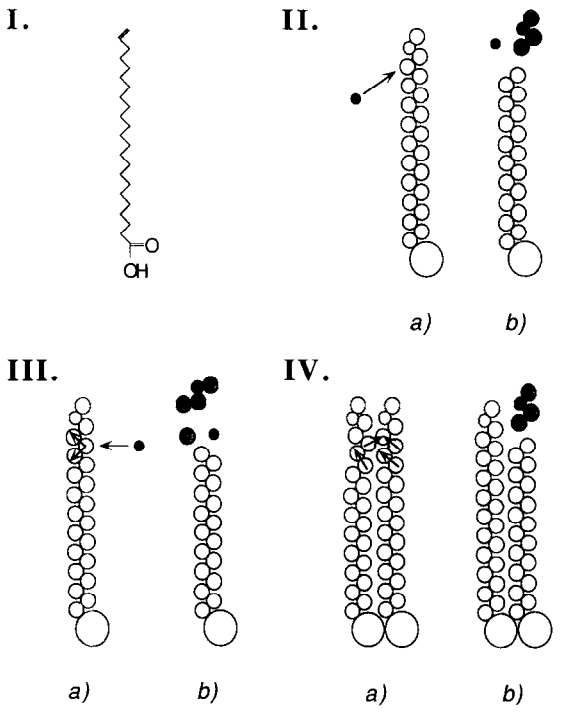

Fig. 1. (I) Chemical structure of the tricosenoic acid molecule (the orientation of the molecule at the surface is respected); (II–IV) Schemes of the different emission pathways for the emission of the original fragment (see text); (II–III) Ejection of a $C_4H_7^+$ resulting from the collision between a cascade atom and the chain; (IV) Ejection of a $C_4H_7^+$ resulting from the vibrational motion of the neighbour atoms.

The remaining, also called relative energy, will constitute the internal energy of the molecule:

$$E_{int} = E - E_{cm} = m_2 E/(m_1 + m_2). \quad (2)$$

These equations show that, for a given momentum transfer, the translational energy term decreases as m_2 increases, whereas the internal energy term increases as m_2 increases.

2.2. polyatomic molecule

In the case of a chain containing n particles, Fig. 1 describes several types of elastic mechanisms leading to the emission of a fragment containing t particles:

(a) the collision between a cascade atom and particle t of the chain, followed by the scission of the nearest C–C bond and the direct emission of the fragment (Fig. 1.II).

(b) the collision between a cascade atom and particle $t+1$ of the chain, followed by the scission of the two adjacent C–C bonds and the subsequent emission of a single particle and a fragment containing t particles (Fig. 1.III).

(c) the scission of the bond following particle t as a result of the vibrational motion of the neighbour atoms (Fig. 1.IV) [17].

In each case, a momentum $\boldsymbol{p}$ (indicated by arrows in Fig. 1) is finally transferred to particle t. Assuming that the energy transferred after bond-breaking to the departing fragment is distributed into the different energy modes as described in Section 2.1, one obtains:

$$E_{cm} = m_t E/M, \tag{3}$$

$$E_{\text{int}} = \sum_{i=1}^{t-1} m_i E/M, \tag{4}$$

where m_i is the mass of particle i, $M = \sum_{i=1}^{I} m_i$ and $E = \boldsymbol{p}^2/2m_t$.

This leads to the important conclusion that for a given momentum $\boldsymbol{p}$, the larger is the fragment, the lower will be its kinetic energy and the greater its internal energy.

For the departing fragment, one can also derive from Eqs. (3) and (4) a direct relation between E_{cm} and E_{int}:

$$E_{cm} = m_t E_{\text{int}} \Big/ \left(\sum_{i=1}^{t-1} m_i \right). \tag{5}$$

2.3. Reorganization of the fragment

The excess energy E_{int}, distributed into the vibrational and rotational energy modes of the fragment, may be sufficient to affect its stability, inducing rearrangement or further fragmentation. Ignoring the detailed physics of the phenomenon, it seems reasonable to consider that a threshold for reorganization exists, and that reorganization occurs when the internal energy of the fragment exceeds this threshold [25]. In first approximation, we assume that the threshold is equal to the formation energy difference between the original fragment and the reorganized fragment states. Then, the energy released for the reorganization can be expressed by the relation:

$$\Delta E_{\text{int}} = \Delta E_{\text{f}}, \tag{6}$$

where ΔE_{f} is the difference of formation energy between the original fragment state and the reorganized species state. In general, the reaction can be a bond-breaking, a rearrangement inside the fragment, etc.

Eqs. (5) and (6) give a threshold for the kinetic energy of the reorganized species:

$$E_{cm}^{\min} = m_t \Delta E_{\text{f}} \Big/ \left(\sum_{i=1}^{t-1} m_i \right). \tag{7}$$

According to this, the threshold for the kinetic energy of the original fragment is zero.

Suppose now that several reorganization pathways exist, with thresholds respectively equal to $\Delta E_{\text{f}}^{(j)}$ ($\Delta E_{\text{f}}^{(j)} < \Delta E_{\text{f}}^{(k)}$ for $j < k$). In this case, the original fragment will produce the reorganized species j if $\Delta E_{\text{f}}^{(j)} \le E_{\text{int}} \le \Delta E_{\text{f}}^{(j+1)}$. Using once more Eqs. (5) and (6), it ensues that the kinetic energy of the reorganized species j has to respect the following inequality:

$$E_{cm}^{(j),\min} = m_t \Delta E_{\text{f}}^{(j)} \Big/ \left(\sum_{i=1}^{t-1} m_i \right) \le E_{cm}^{(j)}$$

$$\le m_t \Delta E_{\text{f}}^{(j+1)} \Big/ \left(\sum_{i=1}^{t-1} m_i \right) = E_{cm}^{(j),\max}. \tag{8}$$

This means that for a given original fragment, the greater is the total energy transmitted, the greater will be the kinetic and the internal energies and the more important the reorganization of the fragment. The species resulting from an important reorganization will thus exhibit a greater mean kinetic energy.

It is important to note that no hypotheses are made in this treatment concerning the distribution of the cascade atoms (or molecules) [6,7] or the spatial distribution of the energy at the surface [26], and that the probability of reorganization is simply equal to 0 or 1, following the quantity of internal energy available. Nevertheless, these simple considerations give characteristic values for the kinetic energy of the secondary species emitted. It will be shown in the following that this model can be applied to the case of the C_xH_y ions sputtered from a tricosenoic acid bilayer, knowing the chemical structure of the chain and assuming favoured pathways for reorganization.

3. Results

The experimental results related to the kinetic energy distributions of the C_xH_y ions sputtered from a tricosenoic acid bilayer deposited on gold have been presented in a previous paper [1]. The effect observed is the following: within a C_iH_y series, the kinetic energy distribution of the ion shifts to higher energies and broadens when the number y of hydrogen atoms decreases. Consequently, the most probable energy and the median of the distribution of saturated ions are lower than those of unsaturated ions (unsaturation effect). This is more pronounced for small clusters (small i), suggesting also an effect of the ion size.

The experimental setup and the principle of the kinetic energy distribution measurement have been described elsewhere [1,24,27]. In this work, measurements using Ga^+ primary ions were reproduced with a slightly different procedure in order to define the curves shape with a better accuracy. In this case, the sample voltage was kept to a fixed value (3 kV) and the energy slit located at the crossover following the first electrostatic analyzer (ESA) of the TRIFT™ time-of-flight spectrometer [27] was shifted perpendicularly to the beam in order to accept different regions of the kinetic energy distribution [24]. For each position, a complete mass spectrum was recorded. Plotting the area of the peak corresponding to a given ion versus

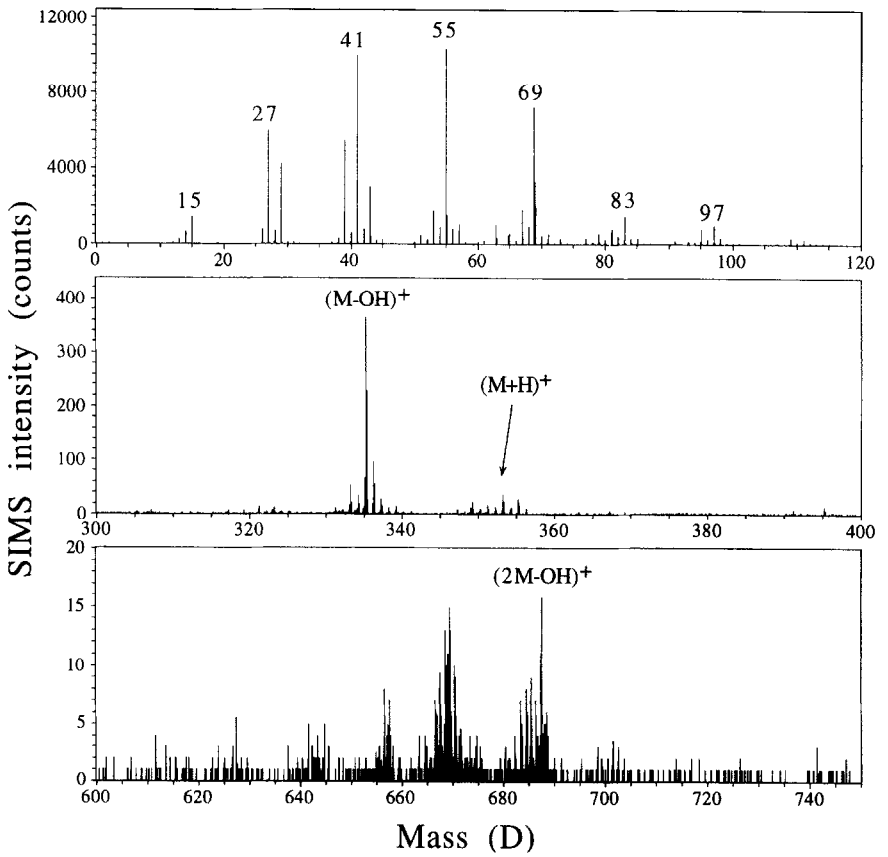

Fig. 2. Positive time-of-flight secondary ion mass spectrum of the tricosenoic acid under (Ga^+, 15 keV) bombardment.

the slit position gave the spatial distribution of this ion after the first ESA. The lateral distribution was then converted into an energy distribution owing to an empirical equation derived from the simulation of the ion trajectories [28]. This procedure does not change the energy resolution (1.5 eV), but it allows a finer tuning of the accepted energy. Indeed, the slit can be shifted continuously, whereas the sample voltage can be increased step by step only in our system (1 eV step).

The positive ion mass spectrum of the tricosenoic acid is shown in Fig. 2. The most characteristic ions appear at masses 353 D $\{(M+H)^+\}$ and 335 D $\{(M-OH)^+\}$, whereas the C_xH_y ions are the most intense peaks below mass 100 D. Fig. 3 shows the kinetic energy distribution of ions CH_3^+ and $C_6H_5^+$. The open circles represent the curves obtained when modifying the sample voltage, whereas the full dots show the curves obtained when moving the slit. As expected, the data corresponding to the two different modes merge onto the same curve, showing that both are equivalent. In addition, the shape of the curve is sufficiently defined to be accurately fitted by an analytical function, which allows an easy determination of the parameters of interest (median, high energy dependence).

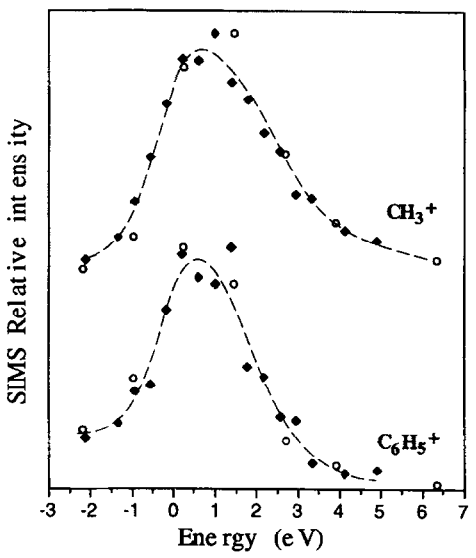

Fig. 3. KED of the ions CH_3^+ and $C_6H_5^+$. The open circles and the full dots show respectively the data obtained when varying the sample voltage and the energy slit position.

Table 1
Formation energy of the $C_xH_y^+$ ions with respect to the formation energy of the original fragment, $C_xH_{2x-1}^+$. (*) indicates the formation energy of the cyclic isomer

Linear isomer	Cyclic isomer *	Mass (D)	ΔE_f (eV)	Linear isomer	Cyclic isomer	Mass (D)	ΔE_f (eV)
C_2^+	–	24	9.2	$C_4H_7^+$	–	55	0
C_2H^+	–	25	6.0				
$C_2H_2^+$	–	26	2.2				
$C_2H_3^+$	–	27	0	$C_5H_4^+$	–	64	5.3
				$C_5H_5^+$		65	3.3/2.5 *
C_3^+	–	36	11.0	$C_5H_6^+$		66	3.1/1.5 *
C_3H^+	–	37	6.7	$C_5H_7^+$		67	1.1/0.2 *
$C_3H_2^+$		38	2.4/4.5 *	$C_5H_8^+$	–	68	1.0
$C_3H_3^+$		39	1.3/2.4 *	$C_5H_9^+$	–	69	0
$C_3H_4^+$		40	1.9				
$C_3H_5^+$		41	0	$C_6H_4^+$		76	6.3 *
				$C_6H_5^+$		77	4.4 *
C_4^+		48	13.9	$C_6H_6^+$		78	6.9/2.8 *
$C_4H_2^+$	–	50	6.0	$C_6H_7^+$		79	4.3/1.5 *
$C_4H_3^+$	–	51	3.9	$C_6H_8^+$		80	4.0/2.0 *
$C_4H_4^+$	–	52	4.0	$C_6H_9^+$		81	2.1/0.9 *
$C_4H_5^+$	–	53	1.9	$C_6H_{10}^+$		82	3.1/1.2 *
$C_4H_6^+$		54	2.2/2.2 *	$C_6H_{11}^+$		83	0 *

Fig. 2 shows that the saturated ions C_xH_{2x+1} (M = 29 D, 43 D, 57 D, etc.) constitute intense peaks in the spectrum. Because of their particular stoichiometry, showing an excess of hydrogen in comparison with the tricosenoic acid chemical structure, the emission of these ions cannot be explained by a direct emission followed by hydrogen elimination, as it is the case for the other C_xH_y ions. For the C_xH_{2x+1} ions, the more probable emission mechanisms are the loss of a carbon atom from a heavier less saturated ion, or the capture of a proton or an hydrogen atom by the departing neutral or ionized fragment. The first possibility implies a rather violent interaction, leading to fragmentation, and seems in disagreement with the very narrow KED of these ions. The second possibility might be the consequence of the reaction with a neighbour molecule during the emission [23]. The resolution of the KED measurement in our system (1.5 eV) is not sufficient to obtain more details about the exact emission process of these ions.

In order to verify the theoretical predictions of Section 2, the median of the KED of the C_xH_y ions ($y \leq 2x-1$), E_{med}, is correlated with the characteristic values E_{cm}^{min}, E_{cm}^{max} calculated for the particular case of the hydrocarbon chain of tricosenoic acid. The chain, $CH_2=CH-(CH_2)_{20}-COOH$, is approximated by a succession of masses separated by chemical bonds, which allows a direct application of Eq. (8) (see Fig. 1). We assume only one reorganization pathway which is hydrogen elimination [5], together with the formation of cyclic structures when they are energetically favoured. The E_f values for $C_xH_y^+$ ions

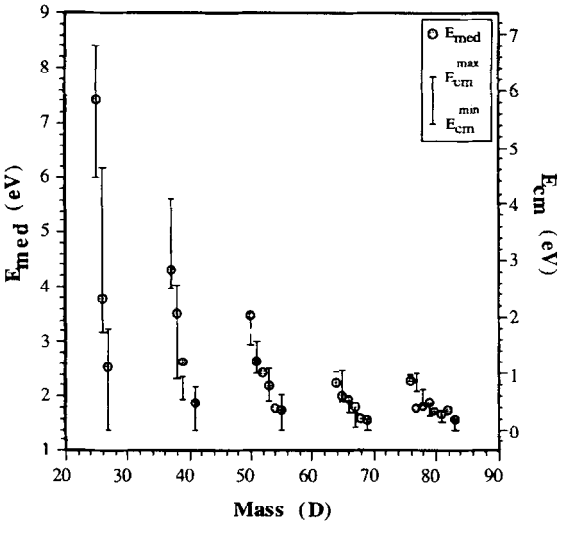

Fig. 4. Median of the KED of the $C_xH_y^+$ ions as a function of the ion mass. The bars indicate the interval between the calculated KE thresholds (E_{cm}^{min}) and maxima (E_{cm}^{max}) (see text).

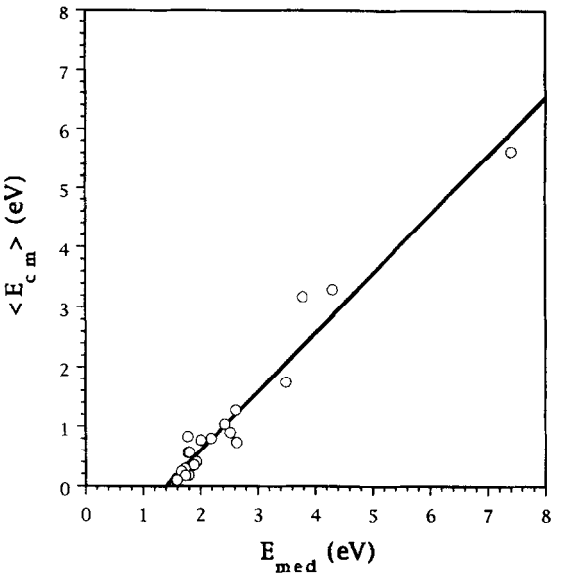

Fig. 5. Correlation between the calculated and experimental characteristic values of the kinetic energy for the $C_xH_y^+$ ions appearing in Fig. 4. The regression line is $\langle E_{cm} \rangle = -1.39 + 0.99\ E_{med}$.

are found in the literature [29], and the ΔE_f are obtained from:

$$\Delta E_f = E_{f.reorganized\ species} - E_{f.original\ fragment}. \quad (9)$$

The ΔE_f corresponding to the reorganized species are indicated in Table 1. These show that the energy required for the reorganization increases with the number of hydrogen atoms released. When they are relevant, the ΔE_f corresponding to cyclic structures are also indicated. In Fig. 4, the experimental and calculated values of the kinetic energy are represented, i.e. the median of the experimental distribution and the characteristic values E_{cm}^{min}, E_{cm}^{max} for each ion in its most stable structure $\{\Delta E_f = \min(\Delta E_{f.cyclic}, \Delta E_{f.linear})\}$, calculated using Eq. (8). There is a good agreement between the two sets of data, suggesting that the transfer of momentum to a carbon atom in the chain followed by the emission and reorganization of the sputtered particle by hydrogen elimination describes appropriately the emission of the $C_xH_y^+$ ions. Fig. 5 shows the quality of the correlation between the experimental values E_{med} and the calculated values $\langle E_{cm} \rangle$, with

$$\langle E_{cm} \rangle = \left(E_{cm}^{min} + E_{cm}^{max}\right)/2. \quad (10)$$

A similar regression can be obtained with the FWHM of the curves instead of the median, with a slope equal to 0.68 and an intercept equal to 1.39. In Fig. 5, the slope of the straight line is close to 1, meaning that $\langle E_{cm} \rangle$ is appropriate to describe the median of the distribution, E_{med}. The value of the intercept (E_{med} = 1.4 eV) is partially due to the limited resolution of the slit (1.5 eV),

but this effect might be also enhanced by a slightly inhomogeneous charge distribution on the sample surface. Indeed, correcting the FWHM of the experimental curves in order to take into account the convolution with the 1.5 eV slit, and plotting it versus $\langle E_{cm} \rangle$ is not sufficient to obtain a zero intercept.

Supported by these results, our interpretation of the emission of the C_xH_y ions can be summarized as follows:

(i) The transfer of momentum to a carbon atom belonging to the molecule of tricosenoic acid induces the scission of the chain and the emission of a hydrocarbon fragment (original fragment). After the bond breaking, the remaining energy is distributed into the 'free' fragment as internal and kinetic energy, the internal energy fraction increasing with the size of the particle. This accounts for the effect of the size observed across the distributions of the C_xH_y ions.

(ii) If the original fragment has an excess of internal energy, it will reorganize mainly by hydrogen elimination, producing a less saturated particle. The result of the reorganization is that the particle releases its excess of internal energy, keeping its kinetic energy nearly unchanged. Therefore, a more important reorganization with respect to the initial chain structure will correspond to a greater kinetic energy of the particle, accounting for the unsaturation effect.

4. Conclusion

A phenomenological interpretation is proposed to account for the observed KED of the secondary ions sputtered from tricosenoic acid under keV bombardment. It is based on the association of collisional and chemical arguments, and gives an insight into the emission and fragmentation processes of molecular organic ions. Hydrogen elimination, together with the formation of cyclic structures, is identified as a favoured pathway for the reorganization of saturated secondary ions with excess internal energy.

On the other hand, this work shows the particular importance of the chemical and molecular structure of the target in the emission process, as it determines the structure of the original fragment from which reorganized species can be produced.

However, these arguments may hardly explain every experimental data related to organic surfaces. In particular, the sputtering of large molecular fragments from polymers [24], involving two bond-breaking, needs the intervention of more complex processes (multiple collision, electronic processes, collision activated chemical reaction, etc.), showing once more that the various interactions resulting from the penetration of the keV primary ion into an organic target lead to several sputtering processes acting in parallel. The elucidation of these fundamental mechanisms seems the more valuable way to achieve quantification in static SIMS.

Acknowledgements

The authors wish to thank Dr. B. Schueler for helpful discussions concerning the experimental part as well as L. Langer and P. Hendlinger for the samples preparation. This work and A. Delcorte's are supported by the Action de Recherche Concertée (94/99-173) of the Communauté Française de Belgique, Direction Générale de l'Enseignement Supérieur et de la Recherche Scientifique. The ToF-SIMS equipment was acquired with the support of the Région Wallonne and FRFC- Loterie Nationale of Belgium.

References

[1] A. Delcorte and P. Bertrand, Proc. ICACS 16, Linz 08/95, Nucl. Instr. and Meth. B. 115 (1996) 246.
[2] G.J. Leggett and J.C. Vickerman, Int. J. Mass Spectrom. Ion Proc. 122 (1992) 281.
[3] S.J. Pachuta and R.J. Cooks, Chem. Rev. 87 (1987) 647.
[4] G. Marletta, S.M. Catalano and S. Pignataro, Surf. Interface Anal. 16 (1990) 407.
[5] A. Delcorte, L.T. Weng and P. Bertrand, Nucl. Instr. and Meth. B 100 (1995) 213.
[6] M.W. Thompson, Philos. Mag. 18 (1968) 377.
[7] P. Sigmund, in: Sputtering by Particle Bombardment I, ed. R. Behrisch (Springer, Berlin, 1981) p. 9.
[8] G. Betz and K. Wien, Int. J. Mass Spectrom. Ion Proc. 140 (1994) 1.
[9] P. Sigmund, H.M. Urbassek and D. Matragrano, Nucl. Instr. and Meth. B 14 (1986) 495.
[10] K. Snowdon, R. Hentschke, W. Heiland and P. Hertel, Z. Phys. A 318 (1984) 261.
[11] K. Snowdon, Nucl. Instr. and Meth. B 9 (1985) 132.
[12] H.M. Urbassek, Nucl. Instr. and Meth. B 18 (1987) 587.
[13] R. Hoogerbrugge and P.G. Kistemaker, Nucl. Instr. and Meth. B 21 (1987) 37.
[14] R.A. Haring, H.E. Rosendaal and P.C. Zalm, Nucl. Instr. and Meth. B 28 (1987) 205.
[15] I.S. Bitensky, Nucl. Instr. and Meth. B 83 (1993) 110.
[16] B.U.R. Sundqvist, Nucl. Instr. and Meth. B 48 (1990) 517.
[17] B.V. King, I.S.T. Tsong and S.H. Lin, Int. J. Mass Spectrom. Ion Proc. 78 (1987) 341.
[18] S.H. Lin, I.S.T. Tsong, A.R. Ziv, M. Szymonski and C.M. Loxton, Phys. Scr. T 6 (1983) 106.
[19] G.M. Lancaster, F. Honda, Y. Fukuda and J.W. Rabalais, J. Am. Chem. Soc. 101 (1979) 1951.
[20] D. Briggs, A. Brown and J.C. Vickerman, Handbook of Static Secondary Ion Mass Spectrometry (SIMS) (Wiley, Chichester, 1989).
[21] R.S. Taylor and B.J. Garrison, Langmuir 11 (1995) 1220.
[22] R.S. Taylor, C.L. Brummel, N. Winograd, B.J. Garrison and J.C. Vickerman, Chem. Phys. Lett. 233 (1995) 575.
[23] R.S. Taylor and B.J. Garrison, Int. J. Mass Spectrom. Ion Proc. 143 (1995) 225.
[24] A. Delcorte and P. Bertrand, presented at SIMS X, Münster 10/95; accepted for publication.
[25] A.W. Kolfschoten, R.A. Haring, A. Haring and A.E. de Vries, J. Appl. Phys. 55 (1984) 3813.

[26] A. Benninghoven, in: Ion Formation from Organic Solids, ed. A. Benninghoven (Springer, Berlin, 1982) p. 77.
[27] B.W.Schueler, Microsc. Microanal. Microstruct. 3 (1992) 119.
[28] B.W. Schueler, private communication.
[29] S.G. Lias, J.E. Bartness, J.F. Liebmann, J.L. Holmes, R.D. Levin and W.G. Mallard, Gas Phase Ion and Neutral Thermochemistry, ed. D.R. Lide Jr (ACS and the American Institute of Physics for the National Bureau of Standards, New York, 1988).